

Tension Testing of Flexible Expansion Joints

Technical Report

Submitted to:

Dennis Shumard
EBAA Iron, Inc.

Prepared by:

H. L. Parnell
L. Guerrero
B. A. Lucero
B. P. Wham



Center for Infrastructure, Energy, and Space Testing
Civil, Environmental, and Architectural Engineering
University of Colorado Boulder
Boulder, CO 80309

July 2020



Table of Contents

Table of Contents	2
List of Figures	3
List of Tables	4
1. Introduction.....	5
1.1 Test Specimens	5
1.2 Test Overview	6
2. Test Setup and Protocols.....	7
2.1 Test Setup.....	7
2.1.1 FEJ Specimen Installation Procedure.....	7
2.1.2 FBFEJ Specimen Installation Procedure.....	8
2.1.3 Instrumentation	9
3. Test Procedure	10
3.1 Pretest.....	10
3.2 Test Sequence	11
3.3 Stop or Pause Criteria	11
4. Results.....	12
4.1 Tension Test FT01 (FEJ) Results.....	12
4.2 Tension Test FT02 (FBFEJ) Results.....	15
4.3 Pressure Test Results	17
4.4 Test Comparisons and Conclusions	19
Acknowledgements.....	21
References.....	21
5. Appendix A: Actuator Lever Force Conversions.....	22
6. Appendix B: Internal Pressure to Axial Force Calculations	24
7. Appendix C: Joint Displacement and Associated Force.....	26



List of Figures

Figure 1.1. Cross-sectional drawing of specimens FT01 and FT02	6
Figure 1.2. Drawing of FEJ specimen in test frame.....	6
Figure 2.1. Drawing of specimens in test frame	8
Figure 2.2. FEJ specimen in test frame.....	9
Figure 2.3. FBFEJ specimen in test frame.....	9
Figure 2.4. Location of string pots as installed on the FEJ.....	10
Figure 2.5. Location of string pots as installed on the FBFEJ.....	10
Figure 4.1. FEJ failure	12
Figure 4.2. FEJ failure at West bell	12
Figure 4.3. Shearing on West retainer ring	12
Figure 4.4. Shearing inside West bell	12
Figure 4.5. FEJ axial force and pressure vs. time	13
Figure 4.6. FEJ force and pressure vs. average specimen displacement.....	13
Figure 4.7. FEJ string pot displacement vs. time	13
Figure 4.8. FEJ string pot displacement vs. actuator displacement	13
Figure 4.9. Tension test FT01 during loading.....	14
Figure 4.10. Initial FBFEJ failure due to bolt shearing at West end.....	15
Figure 4.11. Bolt shearing after completely pulling out joint.....	15
Figure 4.12. Bolt shearing inside West bell.....	15
Figure 4.13. Shearing at West ball joint.....	15
Figure 4.14. FBFEJ (FT02) force, pressure, and applied displacement vs. time	16
Figure 4.15. FBFEJ (FT02) force and pressure vs. applied displacement	16
Figure 4.16. FBFEJ string pot displacement vs. time	16
Figure 4.17. FBFEJ string pot displacement vs. applied displacement.....	16
Figure 4.18. Tension test FT02 during loading.....	17
Figure 4.19. Pressure test 406F20 failure at stop collar.....	18
Figure 4.20. Pressure Test 4406F20B failure at telescoping joint	18
Figure 4.21. Highlighted drawing of 406F20 failure locations.....	19
Figure 4.22. Highlighted drawing of 4406F20B failure locations	20
Figure 4.23. Axial force vs. coupling displacement starting at specimen neutral position.....	20
Figure 4.24. Axial force vs. coupling displacement after engagement of joint	20



Figure 5.1. Pin locations for lever force adjustments..... 22

Figure 6.1. FEJ conversion diameter locations. 24

Figure 6.2. FBFEJ conversion diameter locations. 25

Figure 7.1. FEJ initial pull sequence under zero pressure: force vs. applied displacement..... 27

Figure 7.2. FEJ joint pull prior to coupling engagement (FT01*): axial force vs. (a) time and (b) applied displacement..... 27

Figure 7.3. FBFEJ joint pull (FT01a): axial force vs. (a) time and (b) applied displacement 28

Figure 7.4. FBFEJ joint pull (FT01a): axial force vs. (a) time and (b) applied displacement 28

List of Tables

Table 4.1. Summary of test results..... 19

Table 5.1. Load ratios for the full actuator stroke..... 23

Table 6.1. Equivalent axial force at failure of the FEJ..... 24

Table 6.2. Equivalent axial force at failure of the FBEJ..... 25

Table 7.1. Equivalent axial force at failure of the FBEJ..... 26



1. Introduction

This report is submitted to EBAA Iron, Inc. and presents results from a test program to investigate and compare the axial performance of a Flex-Tend Flexible Expansion Joint (FEJ) and a Force-Balanced Flex-Tend Flexible Expansion Joint (FBFEJ), each nominally 6-in. diameter. Externally applied axial load test results are compared to data obtained from internal pressure burst tests. The work was undertaken in the Center for Infrastructure, Energy, and Space Testing (CIEST) which is affiliated with the Civil, Environmental, and Architectural Engineering Department at the University of Colorado Boulder.

The intention of this study was to test joint specimens for baseline characteristics in axial conditions and to impose external and internal loading conditions to the test specimens that are representative of the significant deformations possible during earthquake-induced ground deformation such as landsliding, fault rupture, and liquefaction-induced lateral spreading, thus characterizing the pipeline system capacity. As detailed, all tests were designed and performed in accordance with procedures and recommendations provided by Wham et al. (2018).

This report is organized into five sections. Section 1 provides introductory remarks, including discussion of test specimens and experimental overview. Section 2 presents test setup and experimental protocols. Section 3 details test procedure for both specimens. Section 4 discusses, compares, and concludes test results. Appendices A-C provide supplementary information and calculations.

1.1 Test Specimens

Flex-Tend units are 6-in. (152-mm) diameter with bell and spigot style expandable joints, equipped with two ball joints capable of 20° of deflection, and are rated up to 350 psi (2.4 MPa). The first specimen (FT01), a series 406F20 Flex-tend Expansion Joint (FEJ), measured 36 ± 2 in. (915 ± 51 mm) at its neutral position from flange to flange. The second specimen (FT02), a series 4406F20B Force Balanced Flex-tend Flexible Expansion Joint (FBFEJ), measured 56 ± 4 in. (1422 ± 102 mm) at its neutral position from flange to flange. The Force Balanced unit has a unique internal design which balances water pressure in an internal chamber, effectively eliminating axial force and associated coupling expansion when internally pressurized. Renderings of each specimen are shown in Figure 1.1 and additional descriptions are provided by Shumard & Teter (2010).

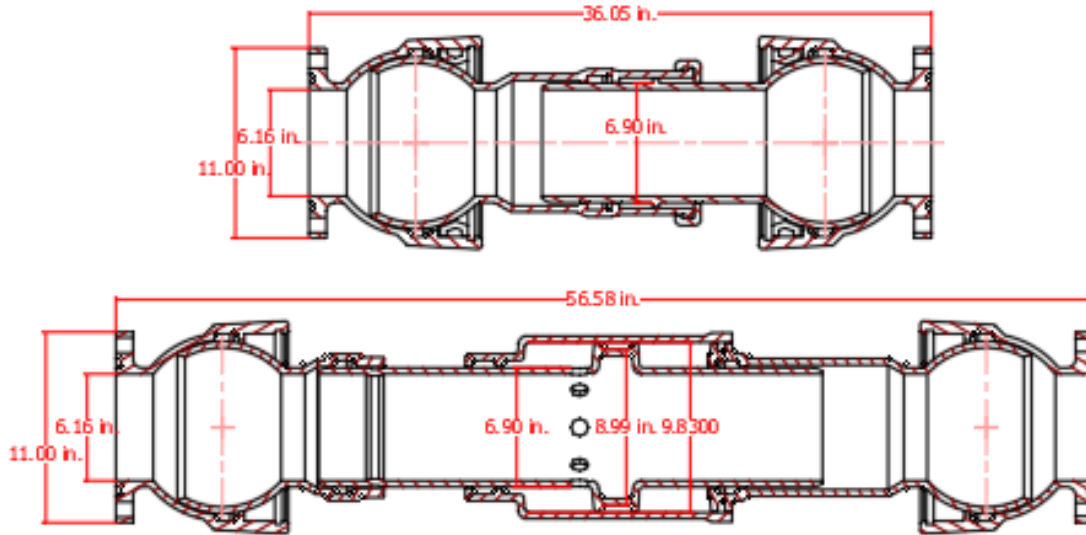


Figure 1.1. Cross-sectional drawing of specimens FT01 and FT02

1.2 Test Overview

Both specimens were tested by CIEST under axial tensile loading while maintaining an internal pressure (equal to laboratory pressure) of 65 psi (448 kPa). A drawing of the axial load test setup is providing in Figure 1.2. Also discussed are the results of internal burst tests on the same style specimens, which were increasingly pressurized to failure. Internal pressure tests were first performed at PSILab, Longmont CO, and were later retested to higher pressure and failure by EBAA.

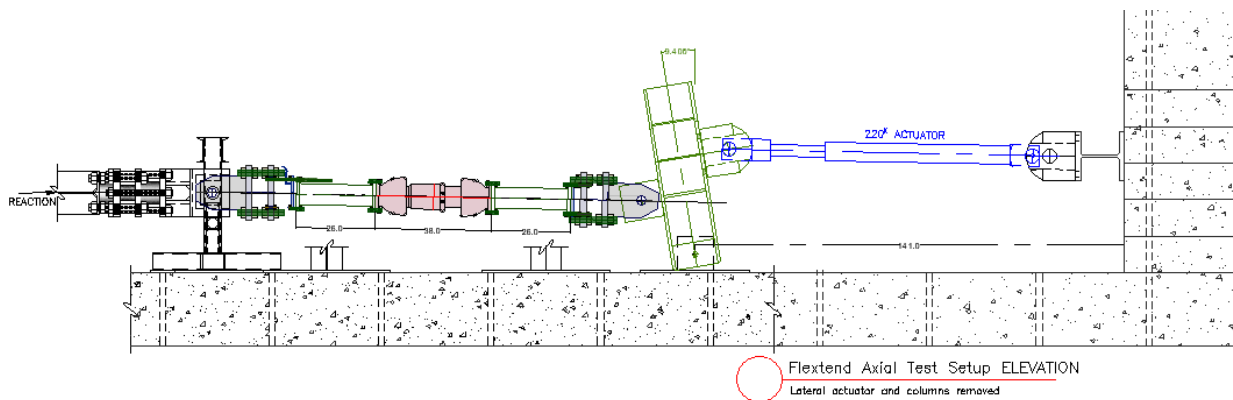


Figure 1.2. Drawing of FEJ specimen in test frame



2. Test Setup and Protocols

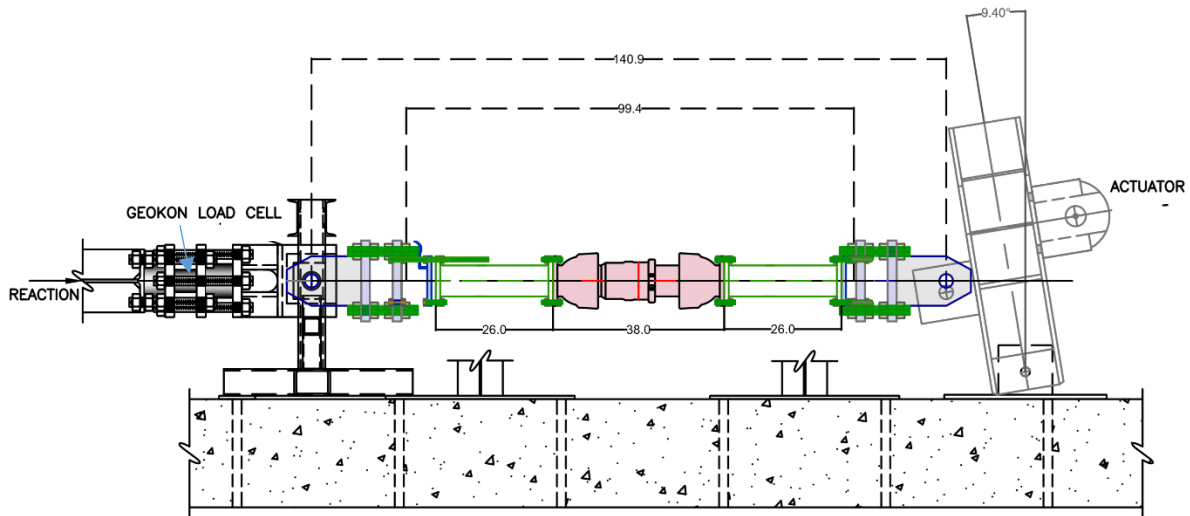
This section is intended to provide a detailed overview of the setup procedure and key experimental constraints associated with application of axial load to the FEJ and FBFEJ Flex-tend joints. The objective is to impose external loading conditions representative of the significant axial loading that can be experienced during earthquake-induced ground motions, ultimately characterizing the axial load capacity of the joint coupling. The reported axial capacity is consistent with earthquake-resistant ductile iron pipe specifications provided by ISO 16143 (International Organization for Standardization, 2006). All tests are designed and performed in accordance with procedures and recommendations provided by Wham et al. (2018).

2.1 Test Setup

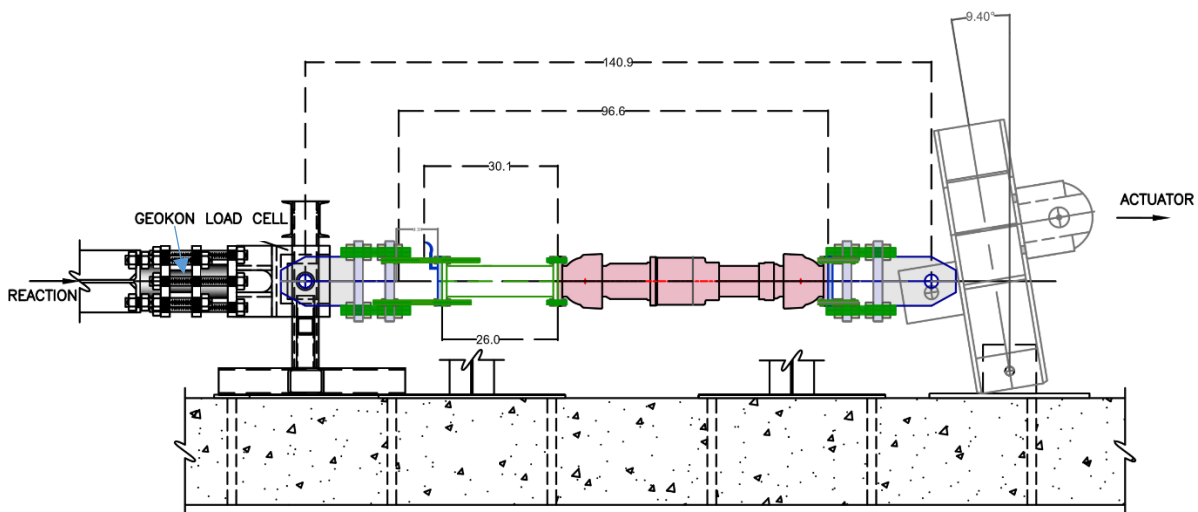
This section outlines the test setup procedure for both specimens. A 244.51S MTS, 220 kip (979 kN) actuator uses a lever system welded to the lab floor and pinned to allow swivel to achieve a maximum of 350 kips (1557 kN) while shortening the actuator stroke from 12 to 6 in. (305 to 152 mm). The system incorporates 26 in. (660 mm) extension pieces. Both sides of the testing apparatus use reaction walls post-tensioned to the strong structures lab floor, as shown in Figure 2.1. A load cell is positioned on the East side, in line with the actuator for redundancy. Plumbing is installed for water input and air release.

2.1.1 FEJ Specimen Installation Procedure

The joint was attached to a 26 in. (660 mm) extension on either side by eight 3/4"-10 high-strength bolts, tightened with a torque wrench to 90 ft-lb (122 Nm). and assembled to the actuator and load cell with eight steel rods. The bleeder valve was oriented to the West end of the test apparatus, closest to the actuator. After attaching the joint, its full expansion capacity was confirmed by pushing the joint to its fully compressed position, indicated by an increase in force on the load cell. Then, the joint was extended fully by pulling until force was detected, indicating point of contact with the stop collar. This position was marked with a yellow line for visual observation during testing. The specimen was then returned to its neutral position of 36 in. (915 mm). The rods and plates were adjusted such that the specimen was straight prior to testing. Starting position of the apparatus can be seen in Figure 2.1.



(a) FT01 (406F20) setup



(b) FT02 (4406F20B) setup

Figure 2.1. Drawing of specimens in test frame

2.1.2 FBFEJ Specimen Installation Procedure

The joint was attached to a 26 in. (660 mm) extension on the East side (opposite the actuator) by eight 3/4"-10 high-strength bolts and assembled to the actuator and load cell with eight steel rods. All fasteners were torqued to 90 ft-lbs., while the threaded rods were wrench tightened due to space restrictions. The bleeder valve was oriented to the East end of the test apparatus. After attaching the joint, its full expansion capacity was confirmed by pushing the joint to its neutral position of 56 in. (1422 mm) without any water inside at a rate of 1 in./min. (25 mm/min.) actuator displacement. Then, the joint was extended fully by pulling until a force was detected, indicating point of contact with the stop collar. Finally, the specimen was returned to



Figure 2.2. FEJ specimen in test frame



Figure 2.3. FBFEJ specimen in test frame

its neutral position of 56 in. (1422 mm). After this dry run, the process was repeated while the joint was full of water at house pressure and data was recorded. The rods and plates were adjusted such that the specimen was straight prior to testing. Starting position of the apparatus can be seen in Figure 2.3.

2.1.3 Instrumentation

Five string pots were installed on each specimen, measuring the distances from outer flange to outer flange, inner flange to inner flange, bell to west flange, bell to spigot, and bell to east flange, as shown in Figure 2.4 and Figure 2.5. A pressure transducer was used to record internal pressure throughout the test. Primary axial load was recorded by the actuator load cell while an inline load cell (Geokon) was included as secondary load measure at the non-actuator side of the setup (Figure 2.1).

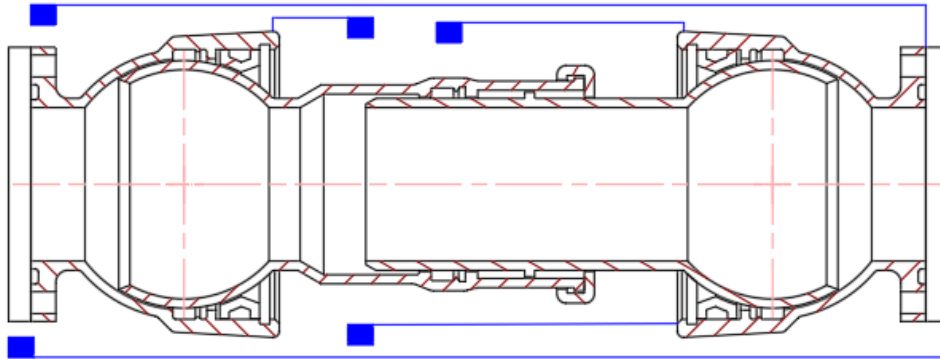


Figure 2.4. Location of string pots as installed on the FEJ.

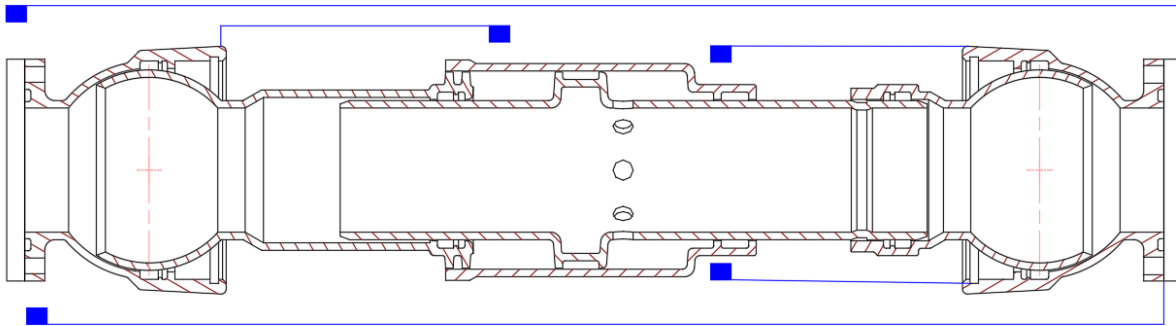


Figure 2.5. Location of string pots as installed on the FBFEJ.

3. Test Procedure

The following section provides details of the test sequence, distributed into three parts: pretest, test sequence, and discussion of pause or stop criteria.

3.1 Pretest

Once the specimens were secured in the loading frame and the calibrated instrumentation installed, the measuring systems were verified and leaks identified by performing and analyzing data from several pressurization sequences. Prior to a pressurization sequence, all nuts were tightened, such that axial pressurization force could be measured by the load cell. The joint was filled with water with the air bleed open. The air bleed was closed once water streamed from it and the system was pressurized to the laboratory pressure of approximately 65 psi (450 kPa), then brought down to 0 psi (0 kPa). This process was repeated multiple times to seat gaskets, verify readings of string pots, and check axial force due to the pressurization



of water. Water was introduced into the specimen more than five hours before testing to ensure thermal acclimation to ambient laboratory conditions. The surrounding testing area was cleared of all tools and other objects and blast shields were placed in appropriate positions. Once ready for the test, a pretest meeting was conducted to review installation conditions, walk through instrumentation locations and expectations, and discuss safety equipment and concerns.

3.2 Test Sequence

After the pretest meeting was conducted and safety concerns addressed, the test sequence was initiated by starting the data acquisition system and laboratory hydraulic systems. A data sampling rate of 4 Hz was used for both tests. The loading nuts at either end of the specimen were tightened to isolate movement to joint expansion. Joint was tested at 65 psi (448 kPa). The test was performed under displacement control at a rate of 1 in./min. (25 mm/min). Displacement was applied until the specimen failed, was no longer capable of holding internal water pressure, or until the maximum stroke of the actuator, 5.26 in. (134 mm) retracted, was reached. Once the test was complete, the data acquisition system was turned off, laboratory hydraulic systems set to low pressure, and data was backed up.

3.3 Stop or Pause Criteria

Several predetermined interruptions to the test sequence were identified prior to testing. The test was paused if the specimen lost all water pressure during the test. If undesirable leakage occurred at the end caps they would be tightened, and the test resumed. If any leakage was observed from the joint, the test would pause briefly, leakage rate assessed, and the test would resume until ultimate failure. The test was paused if any fundamental instrumentation malfunctioned during the test, or if power was lost in any part of the testing laboratory. The test would be terminated when the specimen was unable to hold internal water pressure, which typically occurs as a result of structural failure of the pipe body or connection.



4. Results

The following section presents the results of the axial and pressure tests on both specimens.

4.1 Tension Test FT01 (FEJ) Results

As shown in the post-test images (Figure 4.1 and Figure 4.2), the FEJ specimen failed at the retainer ring of the west ball joint at approximately 99 kips (441 kN). The retainer ring showed signs of shearing as shown in Figure 4.3 and Figure 4.4. Incremental images of the test sequence are provided with description in Figure 4.9.

Figure 4.5 and Figure 4.6 show recorded axial load and internal pressure vs. time and specimen displacement, respectively. Figure 4.7 and Figure 4.8 provide results from various displacement measurements vs. time and actuator displacement, respectively.

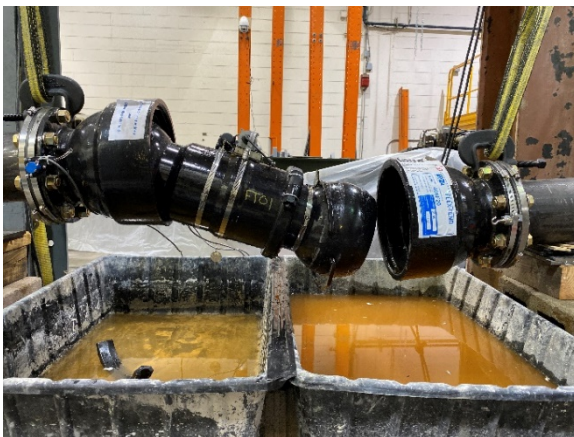


Figure 4.1. FEJ failure



Figure 4.2. FEJ failure at West bell



Figure 4.3. Shearing on West retainer ring



Figure 4.4. Shearing inside West bell

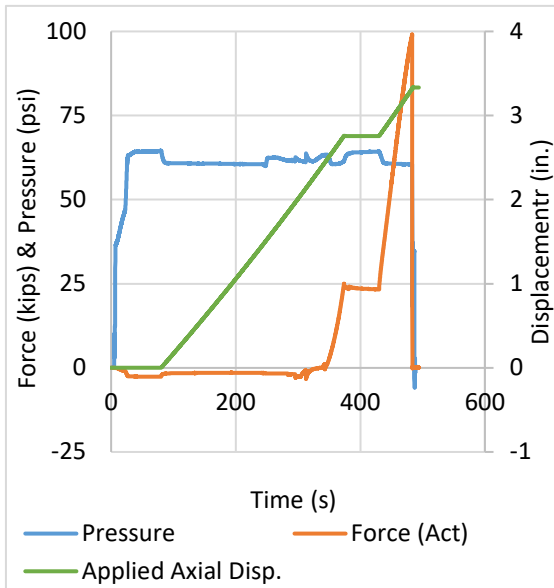


Figure 4.5. FEJ axial force and pressure vs. time

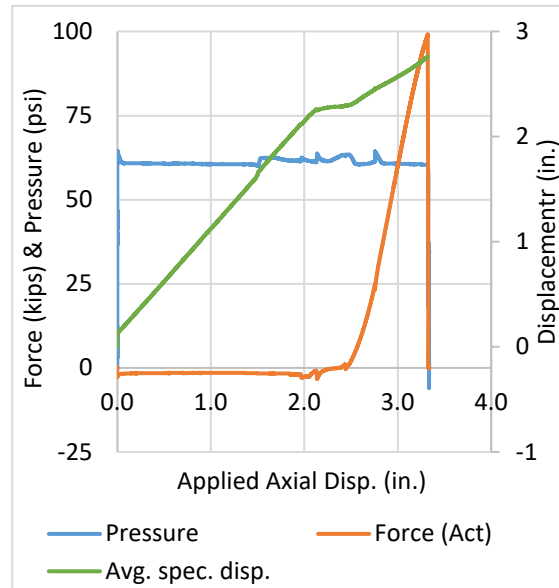


Figure 4.6. FEJ force and pressure vs. average specimen displacement

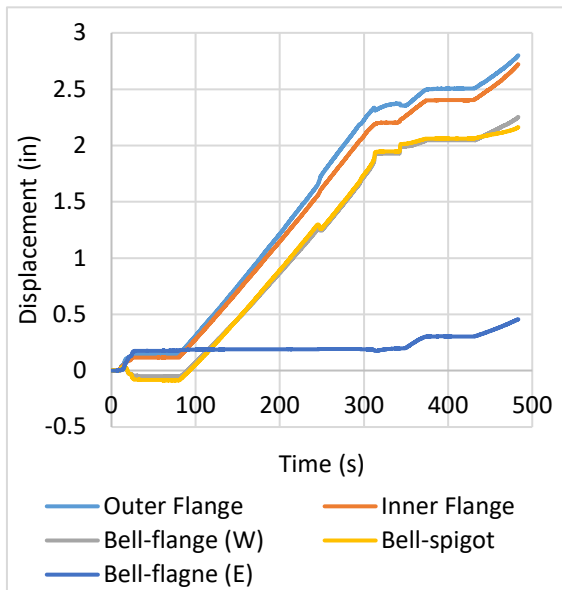


Figure 4.7. FEJ string pot displacement vs. time

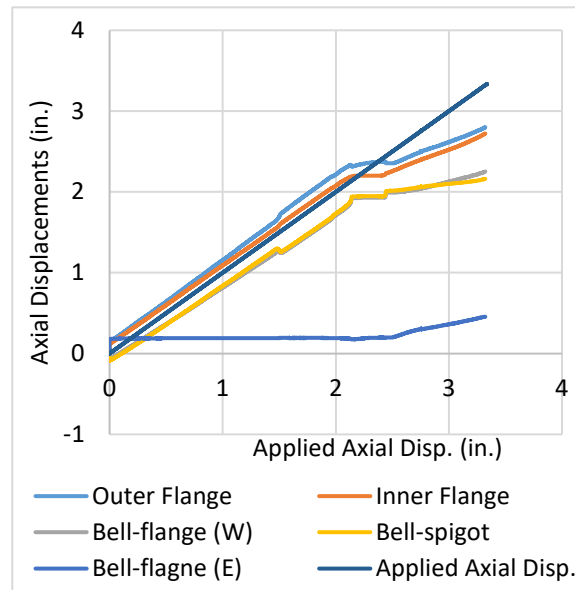
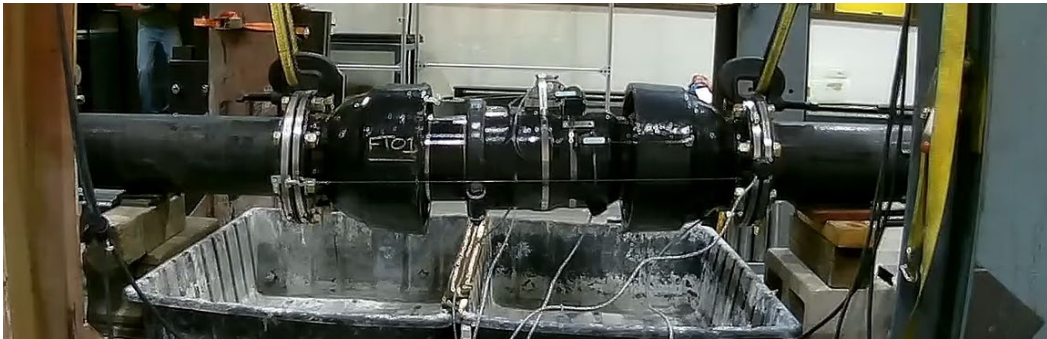
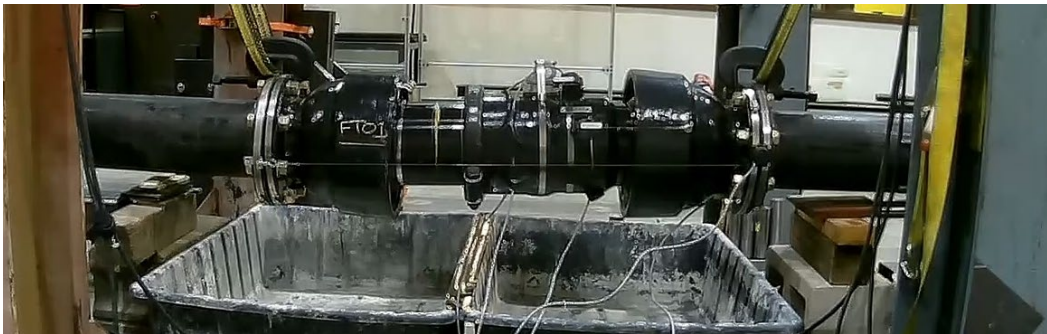


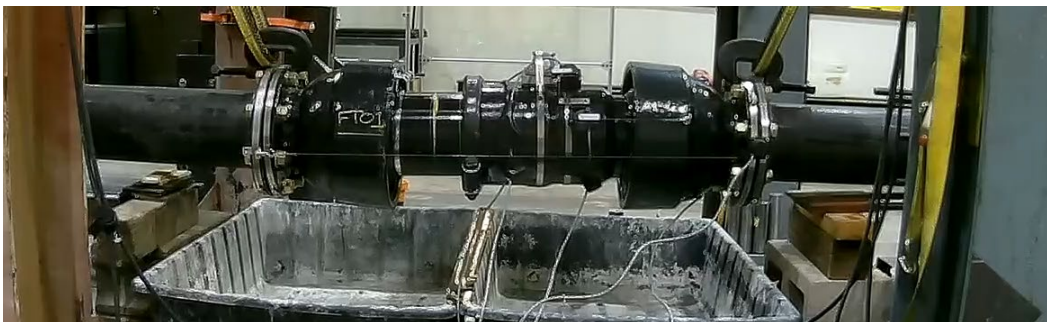
Figure 4.8. FEJ string pot displacement vs. actuator displacement



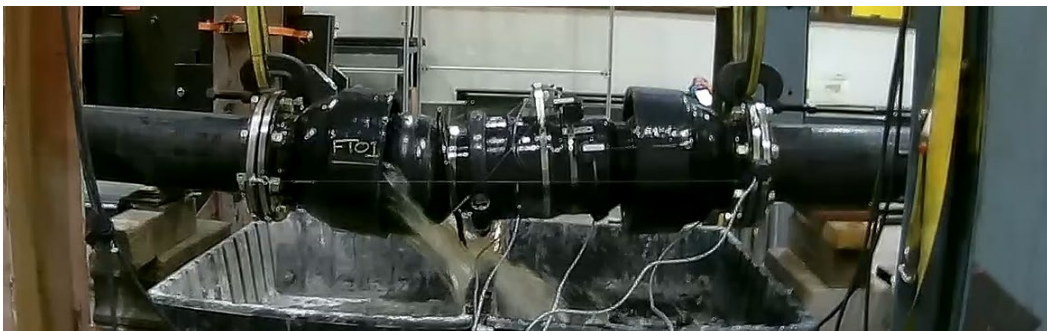
(a) Start of applied displacement



(b) Joint fully extended



(c) Peak force applied



(d) Failure at west ball joint

Figure 4.9. Tension test FT01 during loading



4.2 Tension Test FT02 (FBFEJ) Results

The FBFEJ specimen failed at about 94 kips (420 kN) due to the bolts attaching the west ball to the telescoping joint shearing off and biting into the joint, as in Figure 4.10. The full stroke of the actuator was achieved before specimen failure, so the actuator had to be readjusted before the test could be completed. Despite losing pressure capacity, the joint still had the capacity to hold water after failure but prior to test completion. The actuator was further adjusted at a later day to completely pull apart the specimen.



Figure 4.10. Initial FBFEJ failure due to bolt shearing at West end



Figure 4.11. Bolt shearing after completely pulling out joint



Figure 4.12. Bolt shearing inside West bell



Figure 4.13. Shearing at West ball joint

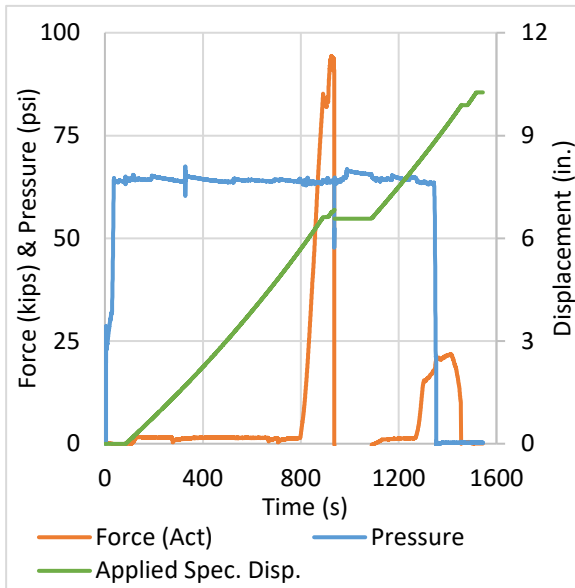


Figure 4.14. FBFEJ (FT02) force, pressure, and applied displacement vs. time

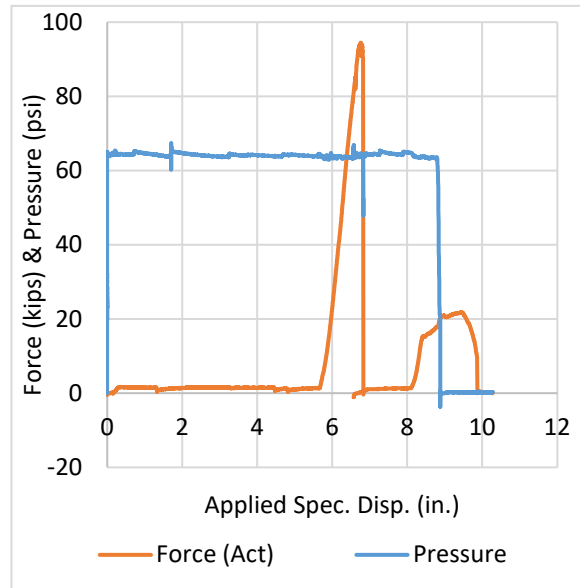


Figure 4.15. FBFEJ (FT02) force and pressure vs. applied displacement

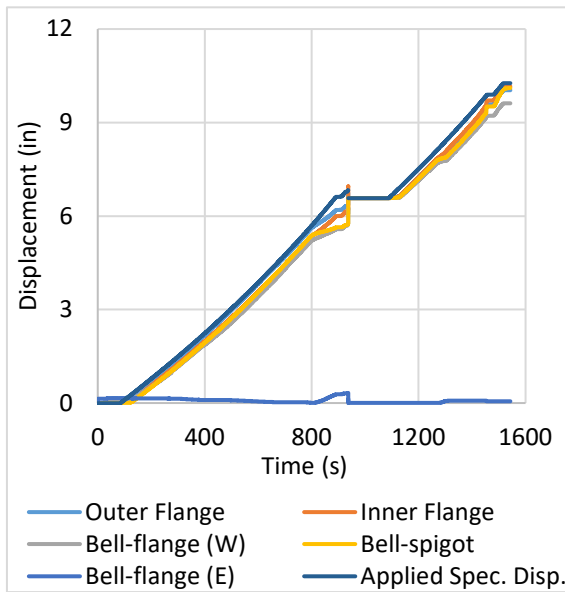


Figure 4.16. FBFEJ string pot displacement vs. time

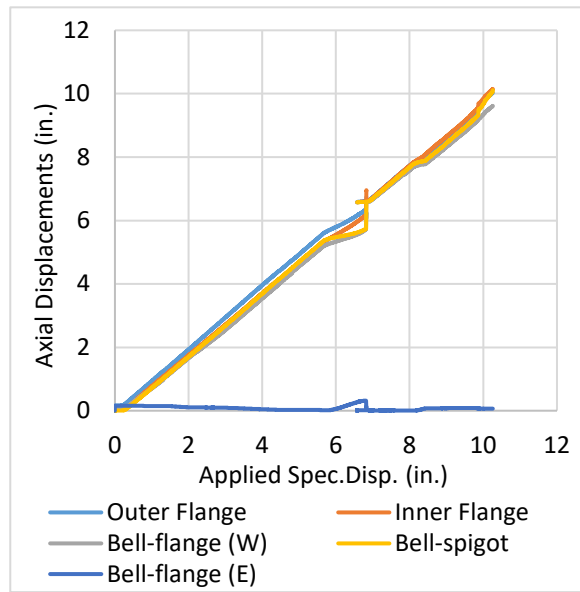


Figure 4.17. FBFEJ string pot displacement vs. applied displacement



a) Start of applied displacement



b) Bolt failure when joint was fully extended



c) Final joint failure at West end



d) Final specimen position

Figure 4.18. Tension test FT02 during loading.

4.3 Pressure Test Results

Application of internal water pressure caused various stresses within the pipe joint, normal to the internal joint components. Many of these stresses were imposed in the circumferential direction, while others imposed axial stress (and force) on the pipe wall. The quantity of applied stress from internal



pressure depends on the internal joint geometry and the joint cross-section of interest. For example, during pressure tests of the 406F20 specimen, failure occurred at the stop collar around the telescoping section of the joint (Figure 4.19). The axial stress applied across the representative cross section is illustrated in Figure 1.1 and is equivalent to the internal pressure multiplied by the cross-sectional area. At this location, a diameter of 6.9 in. is used to calculate this area, based on the joint geometry.



Figure 4.19. Pressure test 406F20 failure at stop collar



Figure 4.20. Pressure Test 4406F20B failure at telescoping joint

The force balanced system is designed such that the joint does not displace axially during pressurization. It uses a chamber around the circumference of the telescoping joint section to counterbalance the axial pressurizing force. At a cross-section taken at the telescoping joint, the area of the pipe (37.4 in^2 , based on a diameter of 6.9 in.) is counterbalanced by the area of the pressurized collar (75.9 in^2), which is depicted in Figure 1.1. While the net result of the pressure balance system is that the joint does not displace, the pipe material between contact surfaces must have adequate strength to transfer the axial stress caused by internal pressure. Considering the internal geometry of the force balanced system, a representative diameter of 6.9 in. was used to calculate cross-sectional area.



4.4 Test Comparisons and Conclusions

The following section compares and draws conclusions on the results of the FEJ and FBFEJ axial and pressure tests, as summarized in Table 4.1. The FEJ specimen axial capacity was 17% lower when tested under internal pressure compare to the axial pull test. The FBFEJ capacity was 21% lower during pressure testing. Additionally, both specimens failed at different locations from each other and from their pressure tested counterparts. The varying failure locations indicate the different stress states imposed by the various loading scenarios on internal joint geometry. Figure 4.21 and Figure 4.22 illustrate the failure locations.

Table 4.1. Summary of test results

Test ID	Test Type	Internal Pressure		Max Axial Force*		Failure Location	Max Act. Disp.	
		psi	MPa	kips	kN		in.	mm
FT01	FEJ Axial Tension	65	0.448	99.1	441	Retainer ring	-0.78	20
PT1a	FEJ Internal Pressure	1922	13.3	71.9*	320	(No failure)	-	-
PT1b ⁺	FEJ Internal Pressure	2200	15.2	82.3*	366	Stop collar	-	-
FT02	FBFEJ Axial Tension	65	0.448	94.4	420	Joint bolts	-5.26	134
PT2a	FBFEJ Internal Pressure	1850	12.8	69.2*	308	(No failure)	-	-
PT2b ⁺	FBFEJ Internal Pressure	2000	13.8	74.8*	334	Stop collar	-	-

*Internal pressure converted to axial force based on diameter of 6.9 in. and cross-sectional area of 37.4 in²

⁺ Test “b” were retests of the same test “a” samples to higher burst pressures.

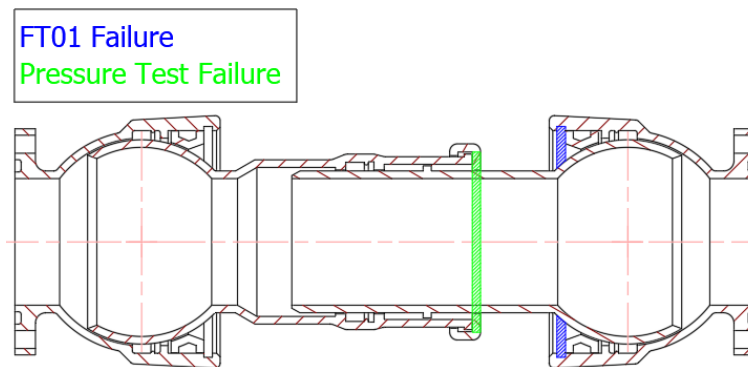


Figure 4.21. Highlighted drawing of 406F20 failure locations

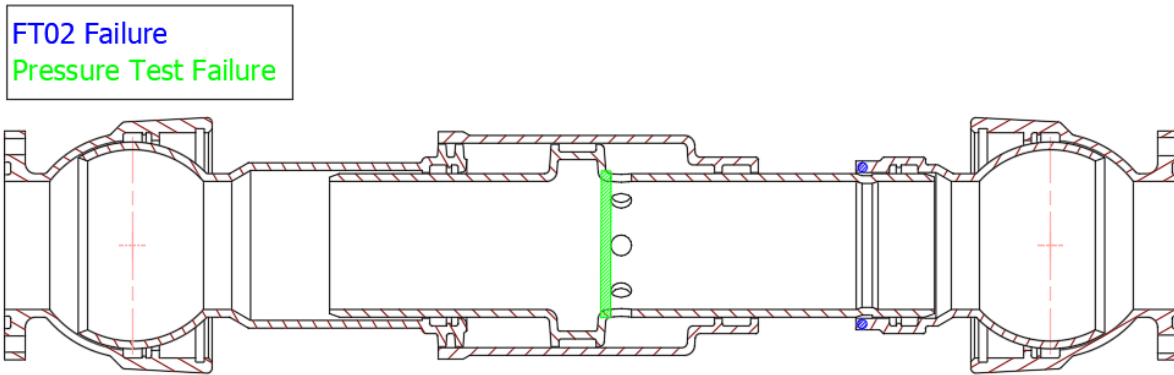


Figure 4.22. Highlighted drawing of 4406F20B failure locations

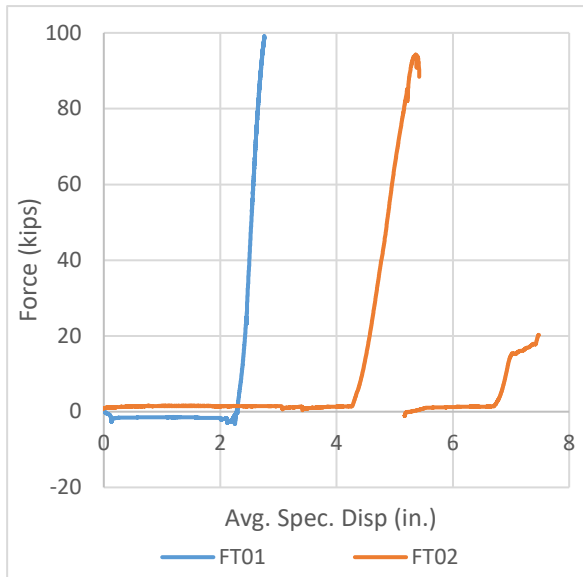


Figure 4.23. Axial force vs. coupling displacement starting at specimen neutral position

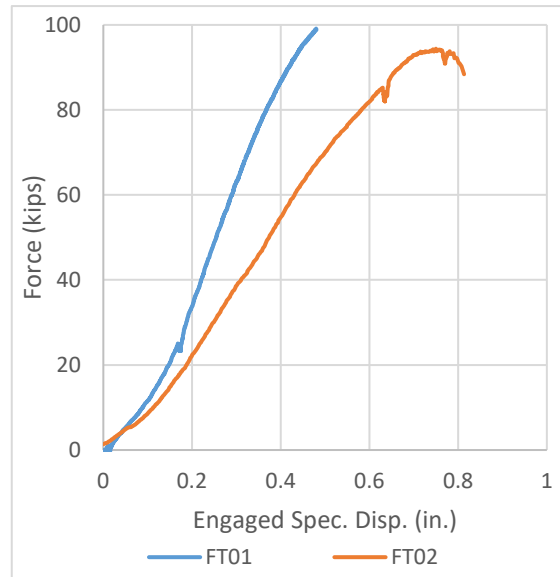


Figure 4.24. Axial force vs. coupling displacement after engagement of joint

The FEJ and FBFEJ exhibited differences in behavior under tensile load. The FEJ specimen (FT01) failed at a slightly higher axial force (99.1 kips vs. 94.4 kips) and exhibited a stiffer response after engagement of the joint in tension, as shown in Figure 4.24. The FBFEJ failed at a slightly lower tensile force and was less stiff, likely attributed to its longer length. Figure 4.23 shows a comparison of results assuming each test started from the coupling's neutral position (center of joint stroke) over the displacement range which the specimens were able to sustain internal water pressure, illustrating the FBFEJ substantial capacity to accommodate axial movement before loss of containment.



The test results provide insight into the seismic tensile capacity of the couplings. Larger axial loads were achieved under axial pull than internal pressure, the former being significantly more representative of earthquake loading in practice. For seismic classification of DI pipe, ISO 16134 suggests that the highest class of earthquake performance is achieved when a pipeline exhibits an axial force capacity of $3D$ (kN) (where D is the diameter of the pipe in mm). For 6 in. (150 mm) diameter pipe this is equivalent to 450 kN, or 102,000 lbs. While each of the couplings tested achieved performance within the $1.5D$ seismic class, the results suggest that the highest class is achievable with minor adjustments to the design of the couplings' internal geometries.

Acknowledgements

The authors wish to recognize the excellent effort of University of Colorado students and staff that made these experiments successful. Namely, the contributions of John Hindman and David Balcells are gratefully acknowledged. Thanks are extended to PSILab for conducting internal pressure tests and to EBAA Iron, Inc. for providing technical and financial support for this project.

References

- EBAA Iron, Inc. *Flex-Tend Flexible Expansion Joint*, EBAA Iron, Inc., 2015.
- EBAA Iron, Inc. *Force Balanced Flex-Tend Flexible Expansion Joint*, EBAA Iron, Inc., 2018.
- International Organization for Standardization (ISO). (2006). *ISO 16134:2006 Earthquake- and subsidence-resistant design of ductile iron pipelines*. Switzerland: ICS: 23.040.10, TC/SC: ISO/TC 5/SC 2. Retrieved from <https://www.iso.org/standard/40651.html>
- Shumard, D., & Teter, J. (2010). "Improved Flexible-Expansion Joint Design Simplifies Pipeline Protection". *Proceedings: Pipelines 2010* (pp. 1217–1228). Reston, VA: American Society of Civil Engineers. doi.org/10.1061/41138(386)117
- Wham, B.P., Berger, B.A., Pariya-Ekkasut, C., O'Rourke, T.D., Stewart, H.E., Bond, T.K., & Argyrou, C. (2018). "Achieving Resilient Water Networks – Experimental Performance Evaluation". *Proceedings: Eleventh U.S. National Conference on Earthquake Engineering* (p. 11). Los Angeles, CA.



5. Appendix A: Actuator Lever Force Conversions

Due to the unique orientation of the lever system, raw actuator forces must be converted by a set of variable factors dependent on actuator position to convert the load cell measurement to equivalent specimen load. Conversions were conducted at three points on the lever system, as labelled in Figure 5.1, where the geometry of the system resulted the need for minor adjustments to the imposed force measure.

The first adjustment accounts for the couple created by the lever itself. Figure 5.1 shows the location of the East and West lever pins, points A and B, respectively. The load ratio is calculated by dividing the East lever pin y-position by the West lever pin y-position (rearranging the sum of the moments equation). Because the pins move in a circular pattern, this load ratio is variable and calculated in a spreadsheet. The next adjustment accounts for the angle between the West actuator pin and the West lever pin (points C and B). This load ratio was calculated by fitting a quadratic model to the angle of the pin relative to the length of the actuator. A similar process was done to account for the angle of the specimen relative to the East lever pin (points D and A). Finally, the three load ratios were multiplied together for a single sum ratio which is multiplied by the raw actuator force to calculate the axial force sustained by the specimen. See Table 5.1 for load ratio values at various intervals along the path of lever rotation. Note the actuator requires minimal adjustment due to pin angle at its neutral (0 in.) position and that the load ratio is maximum when fully extended (5 in.) and minimum when fully retracted (-5 in.).

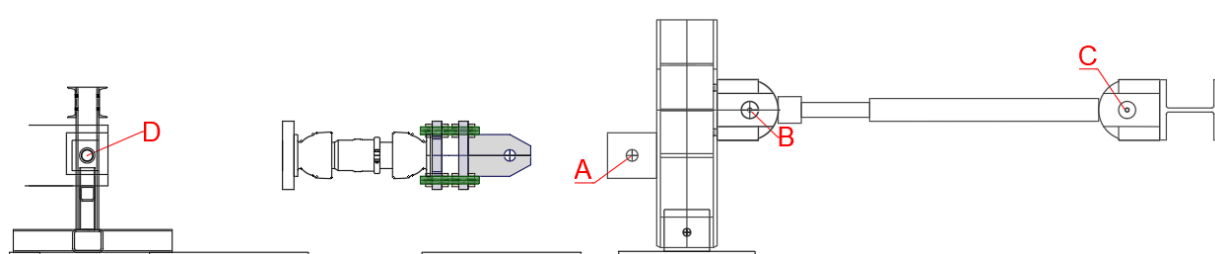


Figure 5.1. Pin locations for lever force adjustments



Table 5.1. Load ratios for the full actuator stroke

Actuator Position (in.)	Moment LR	West LR	East LR	Total LR
5	1.924	0.985	0.984	1.866
4	1.852	0.991	0.990	1.817
3	1.784	0.995	0.994	1.765
2	1.717	0.998	0.997	1.710
1	1.653	0.999	0.999	1.652
0	1.591	1	1	1.591
-1	1.531	0.999	0.999	1.528
-2	1.472	0.996	0.998	1.463
-3	1.414	0.993	0.994	1.396
-4	1.358	0.987	0.990	1.327
-5	1.303	0.981	0.984	1.258



6. Appendix B: Internal Pressure to Axial Force Calculations

To adequately compare the results of the CIEST axial tension tests with the PSILab and EBAA pressure tests, the pressure must be converted to an equivalent axial force based on approximate applied surface area. Note this calculation is an approximate comparison, as internal pressure applies forces to all internal surfaces, which is not practical to precisely account for analytically. Additionally, internal pressure force application is applied to all internal surfaces, as opposed to the forces exhibited by axial testing which are more indicative of loading caused by external forces (e.g., earthquake-induced ground movement). The difference in loading likely accounts for the differences in failure location despite failure forces within 5%. For conversion surface areas, several different locations were considered. Figure 6.1 labels each potential cross-sectional area for the FEJ, while Table 6.1 compares the potential results of conversion based on each.

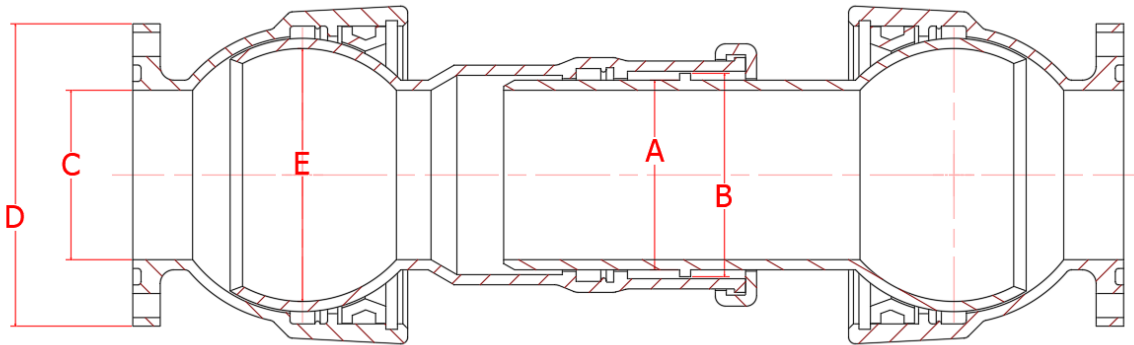


Figure 6.1. FEJ conversion diameter locations.

Table 6.1. Equivalent axial force at failure of the FEJ.

Location	Diameter (in.)	Cross-Sectional Area (in ²)	Converted Force (kips)
A	6.90	37.4	82.3
B	7.40	43.0	94.6
C	6.16	29.8	65.6
D	11.00	95.0	209.0
E	9.20	66.5	146.3
Nominal	6.00	28.3	62.3

The choice to use 37.4 in² (based on the 6.9-in. diameter as denoted by point A in Figure 6.1) was made based on the failure location of CIEST's first axial test on the FEJ, which correlated to that surface area.



For the sake of consistency and simplicity, the decision was made to use the same surface area for the FBFEJ as well. However, it should be noted that the FBFEJ has a more complex anatomy and a few additional surface area conversions, as denoted in Table 6.2 and Figure 6.2.

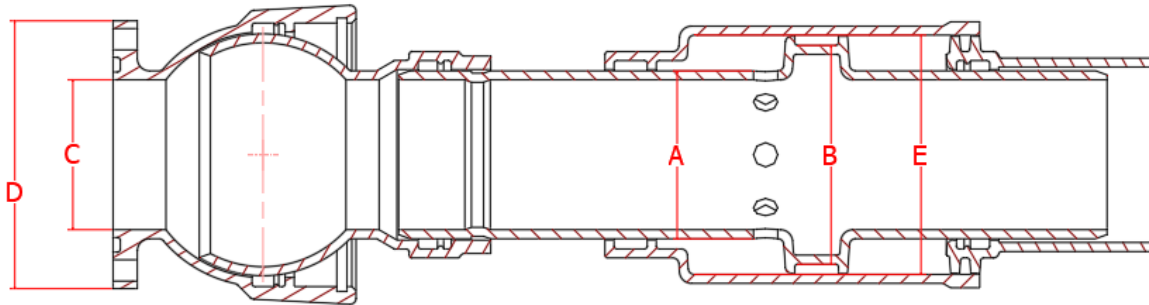


Figure 6.2. FBFEJ conversion diameter locations.

Table 6.2. Equivalent axial force at failure of the FBEJ.

Location	Diameter (in.)	Cross-Sectional Area (in ²)	Converted Force (kips)
A	6.90	37.4	74.8
B	8.99	63.5	127.0
C	6.16	29.8	59.6
D	11.00	95.0	190.0
E	9.83	75.9	151.8
Nominal	6.00	28.3	56.6



7. Appendix C: Joint Displacement and Associated Force

Prior to the axial testing of the FEJ and FBFEJ specimens, the joint expansion capacity of each was affirmed. For the FEJ, this was done while the specimen was full of water but non-pressurized (FT01a). The specimen was pulled from its fully compressed position to fully expanded, the location of which was assumed from a small spike in force read by the load cell. For the FBFEJ, the process was slightly different, and the stroke was tested twice. The first test pull was conducted with no water (FT02a), while the second was with the specimen full of water at house pressure (FT02b). Both times, the specimen was pulled from one inch less than its neutral position to account for actuator displacement capacity to its fully expanded position. Table 7.1 provides a summary of peak forces due to expansion collected by test pulls FT01 and FT02 specimens. Instruments were not recording during FT02a. Figures that follow show the complete test sequences.

Table 7.1. Equivalent axial force at failure of the FBEJ.

Specimen	Test Num.	Test Pull Type	Pressure (psi)	Pull Force (kips)
FT01	FT01a	Wet	0	0.39
FT01	FT01*	Wet	65	0.8
FT02	FT02a	Dry	NA	NA
FT02	FT02b	Wet	65	0.95 – 1.75
FT02	FT02 ⁺	Wet	65	1.5

*Initial pull sequence prior to engagement of coupling for FT01

⁺Initial pull sequence prior to engagement of coupling for FT02

Figure 7.1 shows the FEJ results for FT01, the initial pull sequence performed at zero internal pressure. The pullout force is approximately 390 lb.

Figure 7.2 shows results from the initial joint pull sequence for FT01, prior to FEJ coupling engagement. The dark blue line is the best estimate of axial force to extend the joint. It is the actuator force (yellow) minus the expected force from pressurization (light blue line) assuming a diameter of 6.9 in. Axial pull force under pressure is ~ 800 lbs.

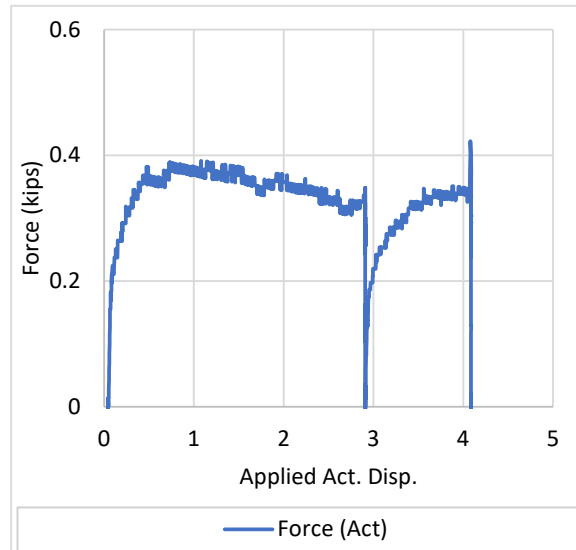


Figure 7.1. FEJ initial pull sequence under zero pressure: force vs. applied displacement

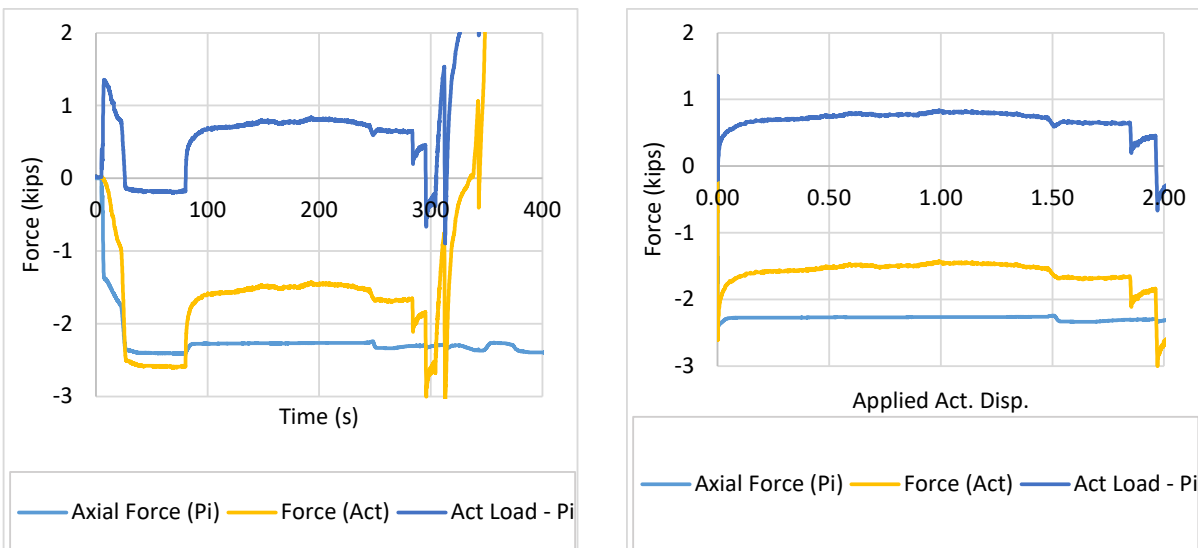


Figure 7.2. FEJ joint pull prior to coupling engagement (FT01*): axial force vs. (a) time and (b) applied displacement

Figure 7.3 provides results from FT02b, the FBFEJ joint opening under 65 psi pressure prior to testing. This test included both an extension of the joint followed by compression back to its approximate starting point. Under extension the recorded force was approximately 1200 lb while under compression the joint force varied from roughly 950 to 1750 lbs. The force in the actuator was not corrected for the axial force due to internal pressure for this sequence because of the internal pressure balancing of the FBFEJ.

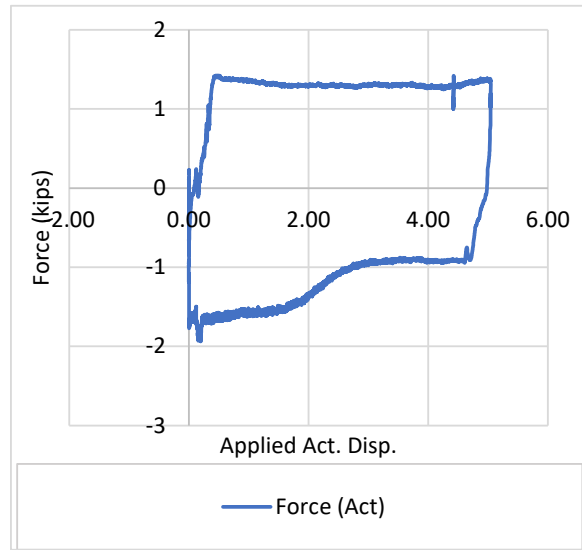
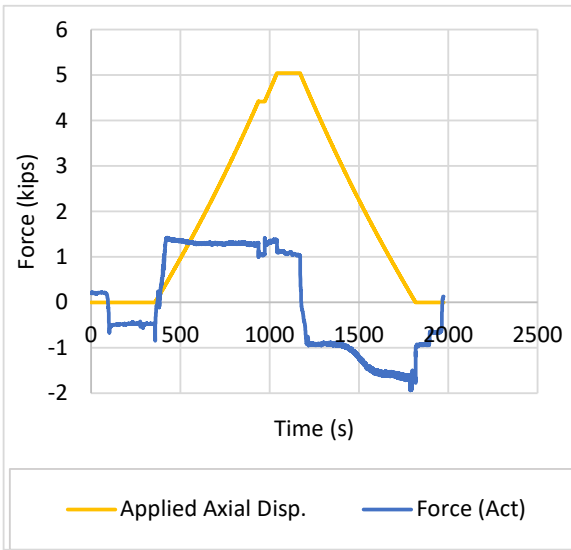


Figure 7.3. FBFEJ joint pull (FT01a): axial force vs. (a) time and (b) applied displacement

Figure 7.4 shows the initial pull sequence for FT02 (FBFEJ) axial tension test. The joint was under 65 psi of water pressure during the ~4 in. joint extension. Pull force required was approximately 1500 lbs.

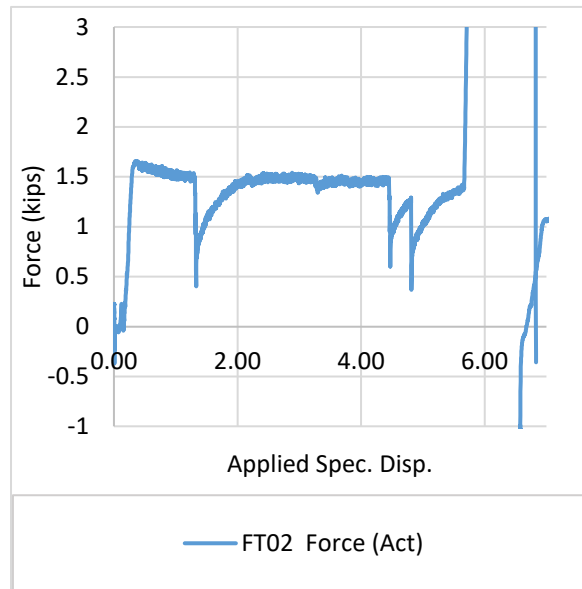
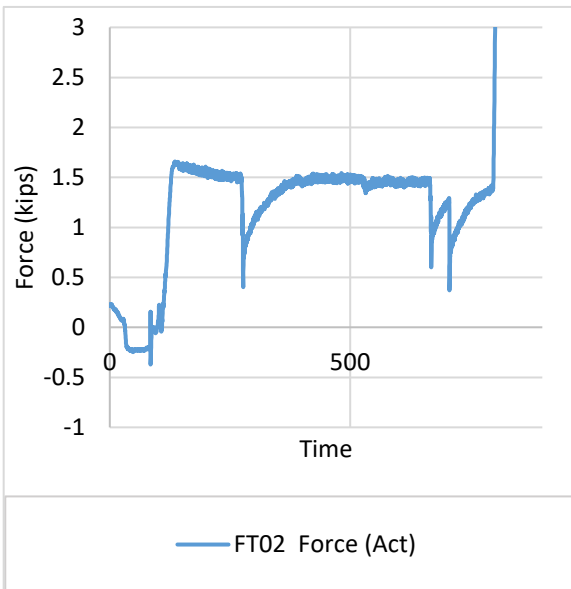


Figure 7.4. FBFEJ joint pull (FT01a): axial force vs. (a) time and (b) applied displacement